



## Linking hydraulic properties of fire-affected soils to infiltration and water repellency

John A. Moody<sup>a,\*</sup>, David A. Kinner<sup>b</sup>, Xavier Úbeda<sup>c</sup>

<sup>a</sup> US Geological Survey, USA

<sup>b</sup> Western Carolina University, USA

<sup>c</sup> University of Barcelona, Spain

### ARTICLE INFO

#### Article history:

Received 10 March 2009

Received in revised form 7 September 2009

Accepted 11 October 2009

This manuscript was handled by P. Baveye, Editor-in-Chief, with the assistance of Juan V. Giraldez, Associate Editor

#### Keywords:

Wildfire

Sorptivity

Hydraulic conductivity

Water repellency

Infiltration

Disk infiltrometer

### SUMMARY

Heat from wildfires can produce a two-layer system composed of extremely dry soil covered by a layer of ash, which when subjected to rainfall, may produce extreme floods. To understand the soil physics controlling runoff for these initial conditions, we used a small, portable disk infiltrometer to measure two hydraulic properties: (1) near-saturated hydraulic conductivity,  $K_f$  and (2) sorptivity,  $S(\theta_i)$ , as a function of initial soil moisture content,  $\theta_i$ , ranging from extremely dry conditions ( $\theta_i < 0.02 \text{ cm}^3 \text{ cm}^{-3}$ ) to near saturation. In the field and in the laboratory replicate measurements were made of ash, reference soils, soils unaffected by fire, and fire-affected soils. Each has a different degrees of water repellency that influences  $K_f$  and  $S(\theta_i)$ .

Values of  $K_f$  ranged from  $4.5 \times 10^{-3}$  to  $53 \times 10^{-3} \text{ cm s}^{-1}$  for ash; from  $0.93 \times 10^{-3}$  to  $130 \times 10^{-3} \text{ cm s}^{-1}$  for reference soils; and from  $0.86 \times 10^{-3}$  to  $3.0 \times 10^{-3} \text{ cm s}^{-1}$ , for soil unaffected by fire, which had the lowest values of  $K_f$ . Measurements indicated that  $S(\theta_i)$  could be represented by an empirical non-linear function of  $\theta_i$  with a sorptivity maximum of  $0.18\text{--}0.20 \text{ cm s}^{-0.5}$ , between  $0.03$  and  $0.08 \text{ cm}^3 \text{ cm}^{-3}$ . This functional form differs from the monotonically decreasing non-linear functions often used to represent  $S(\theta_i)$  for rainfall-runoff modeling. The sorptivity maximum may represent the combined effects of gravity, capillarity, and adsorption in a transitional domain corresponding to extremely dry soil, and moreover, it may explain the observed non-linear behavior, and the critical soil-moisture threshold of water repellent soils. Laboratory measurements of  $K_f$  and  $S(\theta_i)$  are the first for ash and fire-affected soil, but additional measurements are needed of these hydraulic properties for in situ fire-affected soils. They provide insight into water repellency behavior and infiltration under extremely dry conditions. Most importantly, they indicate how existing rainfall-runoff models can be modified to accommodate a possible two-layer system in extremely dry conditions. These modified models can be used to predict floods from burned watersheds under these initial conditions.

Published by Elsevier B.V.

### Introduction

Volume and timing of runoff in infiltration-excess overland flow regimes are controlled by infiltration and thus by the hydraulic properties of the soil, surface boundary conditions, and initial soil moisture conditions. Infiltration can be separated into a short- and a long-time scale response. The short-time scale response depends on the sorptivity-soil moisture relation and reflects the capillary potential and the infiltrability of the soil. The long-time scale response depends on the hydraulic conductivity-soil moisture relation and reflects the gravity potential (Philip, 1957a; Smith, 2002). These relations have been modeled for porous, unsaturated soils by analytical solutions of the Richards' flow equations in 1-D (Philip, 1957a; Smith, 2002), and are easily incorporated into rain-

fall-runoff models. However, these analytical solutions may not represent the actual relations for soils affected by wildfires, which produce volatile chemical compounds, ash, and heat.

The heat impulse into the soil during a wildfire depends primarily on the fuel load and on the duration of the fire. Crown fires, in the canopy layer, with large flame lengths may produce temperatures up to  $1000 \text{ }^\circ\text{C}$  (Ryan, 2002), but may pass quickly and produce less heat flux into the soil than the combustion of the litter and duff layer, which often continue to burn long after a crown fire has passed (Johnson and Miyonishi, 2001). Heat flux into soil during fire can range by several orders of magnitude, and even for a single ecosystem, a wide range of values would be expected. For example, during controlled surface fires in a ponderosa pine ecosystem, the maximum heat fluxes ranged from 2300 to  $3000 \text{ W m}^{-2}$  (Massman et al., 2003). This magnitude of heat flux can drive off adsorbed water contained in the intra-aggregate pores (Blonquist et al., 2006) and reduce the soil moisture content to near zero, producing extremely dry soils.

\* Corresponding author. Address: US Geological Survey, 3215 Marine Street, Suite E-127, Boulder, CO 80303, USA. Tel.: +1 303 541 3011.

E-mail address: [jamoody@usgs.gov](mailto:jamoody@usgs.gov) (J.A. Moody).

Volatile chemical compounds, by-products of combustion, are often hydrophobic. These compounds can penetrate down into the soil through the pore network, and there, in relatively cooler temperatures, condense and coat the surface of particles lining the soil pores and make the soil more water repellent (DeBano, 2000; Doerr et al., 2000; Letey, 2001; Blonquist et al., 2006). Most models of porous media assume “clean” soil particles forming idealized cylindrical pores, but in fire-affected soils, pores may have fire-induced water repellency (in addition to natural water repellency) with a natural pore network that is tortuous with irregular, non-cylindrical walls (Czachor, 2006; Shirtcliffe et al., 2006). These water-repellent compounds and the irregular, non-cylindrical walls will affect the liquid–air–soil contact angle within the pores (King, 1981; Letey et al., 2000; Dekker et al., 2001; Fox et al., 2007), and thus, they influence the sorptivity and hydraulic conductivity that control infiltration into porous media at different soil moisture content (Philip, 1957a; Humphreys and Craig, 1981; Neary et al., 1999; Smith, 2002).

Ash in the broad sense is a mixture of black carbon, soot, and burned organic matter of various size that can include charred material, charcoal, and mineral material transported by the winds created by fire dynamics and deposited as combustion ceases (Jones et al., 1997; Trabaud, 1994). Ash on top of mineral soil produces a two-layer system (Smith, 1990; Kinner and Moody, 2008), and the effects of this two-layer system on the infiltration processes are only beginning to be investigated (Kinner and Moody, 2008; Onda et al., 2008).

For the initial conditions of extremely dry soil, water repellency, and two-layer system, the relations between sorptivity and soil moisture content and between hydraulic conductivity and soil moisture content cannot be assumed to be represented by existing analytical relations used in rainfall–infiltration–runoff models (Brooks and Corey, 1964; Van Genuchten, 1980; Parlange, 1975; Parlange et al., 1985; Smith, 2002; Khlosi et al., 2008). Therefore, the objective of this work was to measure the quantitative relations between sorptivity and hydraulic conductivity and particle size, type of material (soil or ash), and initial soil moisture content (ranging from extremely dry to near saturation); and then use these relations to explain the observed behavior of water repellency.

## Infiltration equations

Infiltration of water into homogenous soil from disk infiltrometers is the combination of gravity-free absorption in three-dimensions (3-D) and gravitational flow downward in one-dimension (1-D) (see Smettem et al. (1994) for discussion). If the flow of air within the soil pores is ignored, and water infiltration is confined by physical boundaries to 1-D, then the gravity-free solution for flow through a horizontal boundary, relates the absorption “depth” or cumulative infiltration,  $I$  [L] to the elapsed time,  $t$  [T], by:

$$I_{1D} = S(\theta_i, \theta_f)t^{1/2} \quad (1)$$

where  $I_{1D}$ , [L], is the equivalent depth of water (if soil was not present), and  $S(\theta_i, \theta_f)$ , [ $LT^{-1/2}$ ], is the sorptivity (Philip, 1957a; Smith, 2002), which represents the ability of soil to absorb water under a suction gradient or pressure potential.  $S(\theta_i, \theta_f)$  is a function of the initial soil moisture content,  $\theta_i$  [ $L^3 L^{-3}$ ], final soil moisture content,  $\theta_f$  [ $L^3 L^{-3}$ ], (which may not equal saturation), and the diffusivity, which is a ratio of the hydraulic conductivity to the water capacity of the soil (Kutílek and Valentová, 1986; White and Sully, 1987; Marshall et al., 1996). In this paper,  $S(\theta_i, \theta_f)$  is replaced by  $S$  to make equations more concise. If gravity is included, then the cumulative infiltration is given by Vandervaere et al. (2000a) as

$$I_{1D} = St^{1/2} + \frac{(2 - \beta)}{3} K_f t \quad (2)$$

Eq. (2) represents the truncation of a power series approximation proposed by Philip (1957b, 1957c) and  $K_f$  [ $LT^{-1}$ ] is the final hydraulic conductivity. Note that  $K_f = K(\theta_f)$  is the hydraulic conductivity at final soil moisture content  $\theta_f$  [ $L^3 L^{-3}$ ] and because disk infiltrometers apply a negative pressure then  $\theta_f$  may be less than saturation. Parameter  $\beta$  is an integral shape parameter such that  $\beta = 0$  corresponds to the Green and Ampt (1911) infiltration equation (Parlange et al., 1985), and typically, is assumed to be about 0.6 (Haverkamp et al., 1994; Vandervaere et al., 2000a). For early times after the beginning of infiltration, the capillary gradient is high and sorptivity controls infiltration (Philip, 1957a). For longer times hydraulic conductivity limits infiltration.

Most 3-D solutions for  $K_f$  and  $S$  require steady conditions or the use of multiple pressure heads. These types of solutions limit the use in remote locations with steep slopes and limited availability of water. Short-time transient solutions are more practical. One transient solution (Smettem et al., 1994; Haverkamp et al., 1994) has the form

$$I_{3D} = St^{1/2} + \left[ \frac{\gamma S^2}{r_d(\theta_f - \theta_i)} + K_i + \frac{2 - \beta}{3} (K_f - K_i) \right] t \quad (3)$$

where  $r_d$  [L] is the disk radius,  $K_i$  [ $LT^{-1}$ ] the hydraulic conductivity  $K(\theta_i)$  at the surface, and  $\gamma$  is a dimensionless proportionality constant introduced by Haverkamp et al. (1994) to correct “for the use of simplified wetting front, sorptivity, and gravity assumptions”. Values of  $\gamma$  have been estimated to be 0.6–0.8 (Haverkamp et al., 1994; Smettem et al., 1995). For dry conditions,  $K_i \ll K_f$ , Eq. (3) simplifies to

$$I_{3D} = St^{1/2} + \left[ \frac{\gamma S^2}{r_d(\theta_f - \theta_i)} + \frac{2 - \beta}{3} K_f \right] t \quad (4)$$

where the first  $S$ -term represents the vertical capillary process, the second  $S$ -term represents the lateral capillary process, and the  $K_f$ -term represents the gravity process (Vandervaere et al., 2000b). For conditions near saturation  $K_i \sim K_f$  and Eq. (3) is approximately

$$I_{3D} = St^{1/2} + \left[ \frac{\gamma S^2}{r_d(\theta_f - \theta_i)} + K_f \right] t \quad (5)$$

## Methods

Most measurements of  $S$  and  $K_f$  were made on a set of soil and ash samples in the laboratory, but some measurements of  $S$  and  $K_f$  were made in the field on soils in burned and unburned areas. All measurements were made using a Mini-disk infiltrometer described later.

## Samples

We developed a set of reference soils, which are intended to serve only as reproducible standards representing ideal soils with uniform particle size. These proposed standards are reproducible such that other researchers can compare hydraulic measurements made on their specific soils with their measurements made on similar reference standards. “Real” soils are composed of mixed particle sizes and a range of organic matter. This makes it difficult, if not impossible, to compare values of  $S$  and  $K_f$  for “real” soils. In addition to acting as standards, measurements of these reference soils provide some insight into the fundamental dependence of sorptivity and hydraulic conductivity on soil moisture content and particle size because the possible dependence on water repellency has

been eliminated (see next paragraph). Values of  $S$  and  $K_f$  for the reference soils reported in this paper are only meant to be used as a standard and to represent an ideal soil. They should not be used to model “real” soils.

Reference soils were obtained from granitic material eroded from the hillslope and recently deposited as small alluvial fans within an area burned by the 2003 Overland Fire near Jamestown, Colorado (Kinner and Moody, 2008). This material was dry sieved and separated into two size classes – silt and clay (<0.063 mm) and very-fine sand (0.063–0.125 mm). These two soil size classes are referred to as “Fine” and “Coarse”, respectively, throughout the remainder of this paper (see Table 1 for sample location, elevation, and soil type). These two soil classes were then further subdivided into two groups to produce four reference soils. The first group was treated by wet sieving, drying, and heating for 1 h at 550 °C to produce a reference soil assumed to have no water repellency (Table 2) because heating above 400 °C destroys water-repellent compounds (Bauters et al., 2000; DeBano, 2000). However, heating at 550 °C caused the disintegration of some soil aggregates so that the material was resieved to eliminate the finer material before infiltration measurements were made. We refer to these soil samples as “Fine, heated reference” or “Coarse, heated reference” soils throughout the paper. These heated reference soils eliminate the complexity introduced by organic matter and its associated water repellency. The second group was the original soil, which probably had some residual water repellency (Table 2) derived from natural sources even though the sieving process probably decreased the degree of water repellency (King, 1981). We referred to these samples as “Fine, natural reference” or “Coarse, natural reference” soils.

Ash and additional soil samples were collected from sites in Colorado and California. Ash samples were collected from the surface on north- and south-facing slopes a few weeks after the 2003 Over-

land Fire area (Table 1), and were separated by sieving into “Fine ash” and “Coarse ash” size classes. Additional surface soil samples were collected from areas burned by the 2000 Hi Meadow Fire near Bailey, Colorado, and from an area burned by the 2005 Harvard Fire near Burbank, California and measured in the laboratory (see Table 1 for location, elevation, and soil types). These samples are referred to as “Burned-lab”. Some soil samples were collected from an unburned area adjacent to the 2000 Hi Meadow Fire and are referred to as “Unburned-lab”.

Replicate in situ measurements were made at sites in Colorado and California. Three measurements were made on the north-facing slope in the area burned by the 2003 Overland Fire (made in 2004), seven in the burned area of the 2000 Hi Meadow Fire (made in 2002), three in the unburned area adjacent to the 2000 Hi Meadow Fire (made in 2002), and three on east-facing and three on west-facing slopes within the boundary of the 2005 Harvard Fire (made in 2005). These measurements were in the same general location as the soil samples that were collected and brought back to the laboratory, and therefore, they had similar elevation and soil type. They are not listed separately in Table 1, but are listed in Table 2 as “Burned-field” or “Unburned-field” samples.

#### Field and laboratory procedures

Laboratory and field measurements of  $S$  and  $K_f$  were made for different soils samples by using the Mini-disk infiltrometer (Decagon Devices; Mini-disk Infiltrator Model S; Decagon, 2006). This infiltrometer (4.4-cm diameter; 32.6-cm tall) is portable, can be easily used on mountain slopes with little water (50–90 mL per measurement), had a variable suction range (–0.5 to –6 cm), and has already been used to make qualitative measurements after some wildfires (Robichaud et al., 2008).

**Table 1**  
Summary information for soil and ash samples (standard error is given as a % following the  $\pm$  symbol).

Descriptor	Center point for sample site, NAD83 Latitude (N) Longitude (W)	Elevation range (m)	Soil type	Particle diameter <sup>a</sup> (mm)	Median diameter (mm)	Bulk density <sup>b</sup> (g cm <sup>-3</sup> ) (%)	Particle density <sup>c</sup> (g cm <sup>-3</sup> )	Porosity	Organic content <sup>d</sup> (%)
<i>Reference soils from the 2003 Overland Fire site near Jamestown, Colorado</i>									
Fine	40° 07.77' 105° 23.65'	2320–2380	Pachic Argiustolls-Aquic Argiudolls	<0.063	–	1.04 ± 2.5	2.14 ± 3.0%	0.52 ± 1.8%	–
Coarse	40° 07.77' 105° 23.65'	2320–2380	Pachic Argiustolls-Aquic Argiudolls	0.063–0.125	0.088	1.16 ± 1.5	2.44 ± 5.7%	0.52 ± 0.6%	–
<i>Soil from the 2003 Overland Fire site near Jamestown, Colorado</i>									
Burned	40° 07.77' 105° 23.65'	2320–2380	Pachic Argiustolls-Aquic Argiudolls	<8.0	0.88 <sup>e</sup> ± 13%	1.10 ± 2.4	~2.4	~0.51	–
<i>Ash from the 2003 Overland Fire site near Jamestown, Colorado</i>									
Fine	40° 07.77' 105° 23.65'	2320–2380	Not applicable	<0.063	–	0.83 ± 2.4	2.44 ± 11%	0.66 ± 1.0%	–
Coarse	40° 07.77' 105° 23.65'	2320–2380	Not applicable	0.063–0.125	0.088	0.79 ± 3.5	1.75 ± 4.9%	0.55 ± 2.0%	–
<i>Soils from the 2000 Hi Meadow Fire site near Bailey, Colorado<sup>f</sup></i>									
Burned	39° 22.30' 105° 22.85'	2495–2500	Typic Usorthents	<6.0	3.7 ± 64%	1.43 ± 1.5	2.48 ± 9.0%	0.42 ± 9.1%	2.1 ± 5.0%
Unburned	39° 22.30' 105° 22.85'	2485–2490	Typic Cryorthents	<1.1	0.76 ± 9.7%	1.27 ± 1.0	2.43 ± 9.6%	0.48 ± 9.6%	4.5 ± 22%
<i>Soils from the 2005 Harvard Fire site near Burbank, California</i>									
Burned	34° 12.86' 118° 17.38'	610–670	Not mapped	<1.48	0.55 ± 8.1%	1.36 ± 5.5	2.34 ± 3.8%	0.43 ± 2.1%	4.3 ± 12%

<sup>a</sup> Size was measured using standard sieves corresponding to whole phi-intervals.

<sup>b</sup> Bulk density was the average of multiple cores that were 3 cm deep (52.05 cm<sup>3</sup>).

<sup>c</sup> Particle density was measured by slowly adding about 0.5–1.6 g to an 8-mm diameter cylinder, agitating the sediment gently to remove air bubbles, and measuring the change in volume. Particle density for 2003 Overland Fire site was estimated based on reference soil from same site.

<sup>d</sup> Organic content was measured as percent loss on ignition after heating for 4 h at 500 °C.

<sup>e</sup> Median particle size was not measured for the specific site but from multiple samples collected within 50 m (see Kinner and Moody (2008), Table 5 for more details).

<sup>f</sup> See Moody et al. (2007b) for more details.

**Table 2**  
Summary of infiltration measurements.

Sample	Water-repellency metric <sup>a</sup>			Mini-disk measurements				Near-saturation hydraulic conductivity, $K_f = K(\theta_f)$		Hydraulic relation: $S = ae^{-b\theta}$		
	Time for 1 mL to infiltrate $T_1$ (s)	Soil moisture ( $\text{cm}^3 \text{cm}^{-3}$ )	Number	Type	Number	Pressure head (cm)	Minimum $R^2$ for fits to Eq. (2), (4)	Mean ( $\text{cm s}^{-1}$ )	Standard error (%)	a ( $\text{cm s}^{-0.5}$ )	b	$R^2$
<i>Reference soil</i>												
Fine, heated	1.2	0.0043	4	3-D	19	−6	0.997	$12 \times 10^{-3}$	14	0.17	2.5	0.62
Fine, heated	2.4	0.0019	4	1-D	20 <sup>b</sup>	−6	0.997	$4.3 \times 10^{-3}$	11	0.17	2.3	0.45
Fine, natural	4.2	0.0095	2	1-D	12	−6	0.994	$0.93 \times 10^{-3}$	11	0.10	9.1	0.91
Coarse, heated	0.4	0.0025	7	3-D	26	−6	0.995	$130 \times 10^{-3}$	16	0.23	3.5	0.77
Coarse, heated	2.0	0.0025	6	1-D	22	−6	0.910	$3.8 \times 10^{-3}$	26	0.20	5.0	0.71
Coarse, natural	2.5	0.0086	2	1-D	24	−6	0.994	$1.8 \times 10^{-3}$	9.6	0.067	8.5	0.42
<i>Ash</i>												
Fine	1.7	0.0023	2	3-D	11	−6	0.998	$12 \times 10^{-3}$	17	0.14	4.4	0.85
Fine	3.6	0.0155	1	1-D	10	−6	0.998	$4.5 \times 10^{-3}$	9.0	0.053	3.1	0.20
Coarse	0.6	0.0046	2	3-D	10	−6	0.996	$53 \times 10^{-3}$	38	0.24	6.8	0.94
<i>Overland Soil</i>												
Burned-field	4.9	0.0204	3	3-D	3	−6	0.999	Measurement calculation produced negative values		Insufficient data		
<i>Hi Meadow soil</i>												
Burned-field	2.7	0.013 <sup>c</sup>	7	3-D	Made with Mini-disk model_0.5 on 16 August 2002							
Burned-lab	5.4	0.0188	3	3-D	8	−2	0.999	$2.0 \times 10^{-3}$	24	0.066	20.3	0.65
Burned-lab	4.9	0.0027	2	1-D	12	−2	0.992	$1.9 \times 10^{-3}$	66	0.082	56.1	0.90
Unburned-field	41	0.031 <sup>c</sup>	3	3-D	Made with Mini-disk model_0.5 on 16 August 2002							
Unburned-lab	16	0.0104	2	3-D	15	−4	0.992	$3.0 \times 10^{-3}$	22	Constant $\sim 0.016 \text{ cm s}^{-0.5}$		
Unburned-lab	19	0.0124	2	1-D	10	−4	0.981	$0.86 \times 10^{-3}$	16	Constant $\sim 0.010 \text{ cm s}^{-0.5}$		
<i>Harvard soil</i>												
Burned-field	72	0.012	6	3-D	6	−6	0.993	$1.3 \times 10^{-3}$	18	Insufficient data		
Burned-lab	7.2	0.010	6	3-D	15	−2	0.987	$7.7 \times 10^{-3}$	18	0.11	16.3	0.74
Burned-lab	5.6	0.014	2	1-D	10	−2	0.991	$1.1 \times 10^{-3}$	24	0.078	22.5	0.54

<sup>a</sup> Volume of water that infiltrated in 30 s was interpolated or extrapolated from the data and then converted to a time to infiltrate 1 mL.

<sup>b</sup> Two runs at  $\theta_i/\theta_f = 0.81$  had no infiltration after about 10 min.

<sup>c</sup> See Moody et al. (2007b) for soil moistures in Tables 7 and 8 for 16 August 2002.

For comparison purposes, we measured a water-repellency metric in the field and before any laboratory sample processing or repeated infiltration measurements altered the water repellency (King, 1981; Doerr et al., 2000). We modified the metric proposed by Robichaud et al. (2008), who suggested using the volume of water that infiltrates into the soil in 1 min. We measured the volume that infiltrated in 30 s (because for some samples the entire capacity, ~90 mL, of the Mini-disk infiltrated in less than 1 min), and calculated the water-repellency metric as the time,  $T_r$ , for 1 mL of water to infiltrate into a soil sample (Table 2). This water-repellency metric depends on soil moisture content (Doerr et al., 2000), so we have reported the metric corresponding to dry soil moisture conditions ( $<0.03 \text{ cm}^3 \text{ cm}^{-3}$ ). Soil moisture could not be controlled in the field, but in each case the metrics corresponded to dry soil conditions (Table 2). This metric intuitively reflects the degree of water repellency (i.e. longer times would correspond to a greater degree of water repellency), and thus, is similar to the water drop penetration time (WDPT) metric, which is a measure of the persistence of water repellency (Doerr, 1998; Letey et al., 2000; Robichaud et al., 2008).

Initial and final soil moisture contents were determined for all measurements. A 3-cm deep soil core with a volume of  $52.05 \text{ cm}^3$  was collected before and after each measurement in the field and in the laboratory. In the field, “before samples” were collected outside the potential wetted area, and in the laboratory, “before samples” were collected from soil used to fill the experimental cylinders described below. “After samples” were collected from the soil directly under the Mini-disk infiltrometer. Samples were put in sealed soil cans, weighed, dried at  $105^\circ\text{C}$ , and reweighed to determine the mass of water lost and mass of dry sediment. Soil moisture content based on mass data were then converted to volume using the soil bulk density (Table 1).

Field measurements using the Mini-disk infiltrometer on steep, burned slopes had some problems to keep in mind. For some measurements, water moved almost completely laterally rather than vertically. Excavation after some measurements found a layer just beneath the soil surface that appeared to be ash, and some measurements appeared to lack a good seal between the disk and the Coarse textured soil on a steep surface. Thus, it is important to

compute the values of  $S$  and  $K_f$  in the field so that changes can be made immediately rather than discovering problems later. Moreover, it emphasizes the necessity to examine the subsurface to determine if the experiment meets the assumptions of Eqs. (3)–(5). Field measurements of  $K_f$  were made only in the Harvard and Overland Fire sites, and all 3-D field measurements were made at dry soil conditions ( $\theta_i = 0.0089\text{--}0.019 \text{ cm}^3 \text{ cm}^{-3}$  and  $\theta_i = 0.017\text{--}0.025 \text{ cm}^3 \text{ cm}^{-3}$ , respectively); therefore, the entire  $S\text{--}\theta$  relation could not be determined in the field.

Laboratory measurements have the advantage of permitting replicate measurements over a wide range of predetermined initial soil moisture conditions not possible in the field. However, the disadvantage is that measurements are made on disturbed soils and repeated wetting and drying may affect the water repellency. Soil samples were collected from the field, oven dried at  $105^\circ\text{C}$ , resieved, and then predetermined volumes of water were mixed uniformly into the soil to produce the desired initial soil moisture content. Cumulative infiltration was measured under 3-D conditions and under conditions approximating 1-D infiltration; we refer to these as 3-D and 1-D measurements throughout this paper although all infiltration measurements are technically made in 3-D. For 1-D infiltration measurements, soil was introduced in 5–10 increments into a 5.1-cm diameter, 20-cm tall cylinders with porous landscape fabric and wire screening on the bottom to allow air to escape but retain the soil sample. These cylinders were about 1 mm larger than the diameter of the base of the Mini-disk infiltrometer. Increments of soil were placed inside the cylinder and tamped gently using a hand piston by the same person for each set of measurements. The full, packed cylinder was covered with an aluminum sheet, until the measurements were made, to avoid loss of moisture. For 3-D infiltration measurements, soil samples were prepared using the same technique, but put in 10-cm diameter, 12-cm tall plastic cylinders. The 10-cm diameter was large enough so that the cylinder walls did not visibly affect the 3-D shape of the wetting front during infiltration except near the end of a few measurements. Soil samples were redried after each infiltration measurement and reused for the next measurement at different initial soil moisture content.

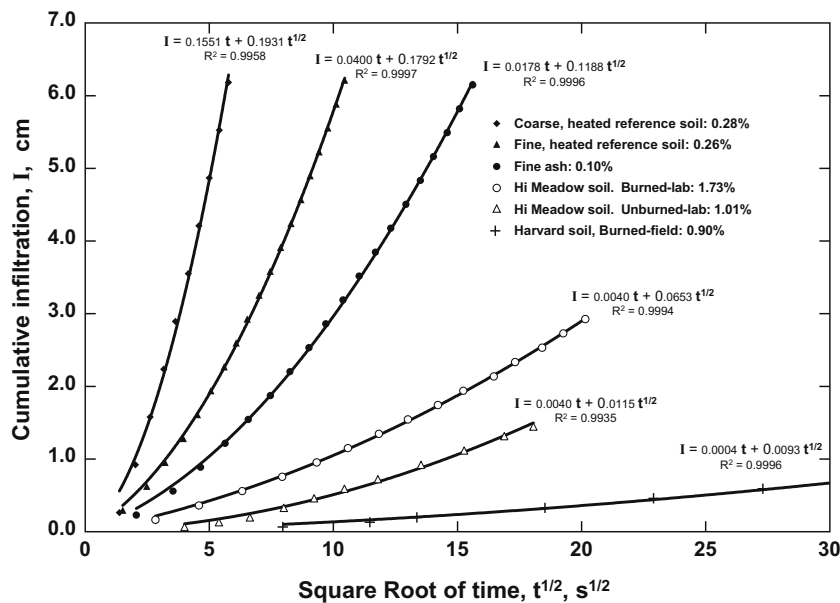


**Fig. 1.** Selected examples of 3-D infiltration measurements for different types of material. Each was selected to represent dry, initial soil moisture conditions and the soil moisture (% by volume) is listed in the explanation. The coefficient of  $t^{1/2}$ -term is the sorptivity value in  $\text{cm s}^{-1/2}$ . The coefficient of the  $t$ -term is used to calculate hydraulic conductivity.

Determination of  $S$  and  $K_f$

Cumulative infiltration,  $I$ , as a function of elapsed time,  $t$ , was measured for different values of  $\theta_i$ . The results ( $I$  and  $t$ ) were fit, using least-squares regression, to a second-order polynomial having the form  $I = At^{1/2} + B(t^{1/2})^2$  (Fig. 1). For 1-D measurements Eq. (2) was used, giving

$$S = A \tag{6}$$

and

$$K_f = \frac{3B}{2 - \beta} \tag{7}$$

For 3-D measurements and relatively dry conditions,  $\theta_i/\theta_f \leq 0.5$ , Eq. (4) was used, giving Eq. (6) above, and

$$K_f = \left(\frac{3}{2 - \beta}\right) \left[ B - \frac{\gamma S^2}{r_d(\theta_f - \theta_i)} \right] \tag{8}$$

For 3-D measurements and conditions near saturation,  $\theta_i/\theta_f > 0.5$ , Eq. (5) was used, which also gave Eq. (6) and

$$K_f = \left[ B - \frac{\gamma S^2}{r_d(\theta_f - \theta_i)} \right] \tag{9}$$

Results

Cumulative infiltration data collected using the Mini-disk infiltrometer consistently fit a second-order polynomial with coefficient of regression for all experimental runs greater than 0.91 and most greater than 0.98 (see examples in Fig. 1). Thus, values of sorptivity,  $S$ , were well constrained whereas values of hydraulic

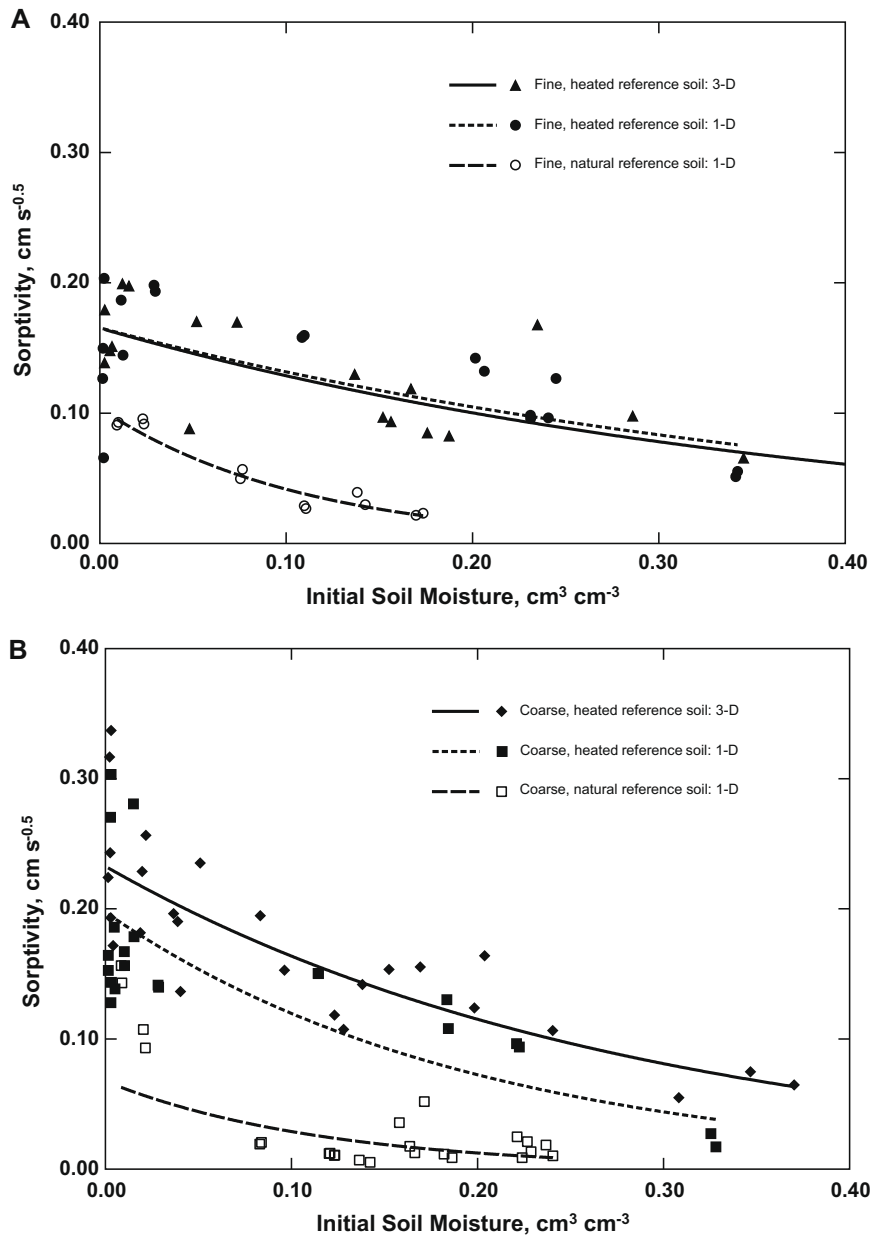


Fig. 2. Sorptivity as function of initial soil moisture content for heated and natural reference soils, for one- and three-dimensional (1-D and 3-D) infiltrometer measurements, and for two particle size classes. (A) Fine represents particle diameter: <0.063 mm and (B) Coarse represents particle diameter: 0.063–0.125 mm.

conductivity,  $K_f$ , depended on the choice of  $\beta$  and  $\gamma$ . The dependence of cumulative infiltration on sorptivity can easily be seen in Fig. 1 as the coefficient  $A = S$  decreases by three orders of magnitude, and the length of time for 1 cm of water to infiltrate (proportion to the water-repelleny metric,  $T_1$ ) increases substantially.

**Sorptivity**

Sorptivity decreased exponentially as a function of  $\theta_i$  for the 1-D and 3-D measurements of both heated reference soils. The  $S$ - $\theta$  relations had the form:

$$S = ae^{-b\theta_i} \tag{10}$$

For soil moisture content near zero ( $\theta_i < 0.02 \text{ cm}^3 \text{ cm}^{-3}$ ), the sorptivity of the Fine, heated reference soils (Fig. 2A) was significantly less ( $p = 0.014$ , 3-D measurement) than the Coarse, heated reference soils (Fig. 2B) (insufficient data for a 1-D t-test; two-tailed, t-test are used throughout). Similar exponential relations (Eq. (10), Table 2) were measured for both natural reference soils, but sorptivity measurements (1-D) were about half ( $0.005$ – $0.156 \text{ cm s}^{-0.5}$ ) those measured for heated reference soils ( $0.027$ – $0.303 \text{ cm s}^{-0.5}$ ) (Fig. 2A and B).

For ash, the  $S$ - $\theta$  relation was also an exponential function. Fine ash and Coarse ash had similar values of  $a$  ( $0.14$  and  $0.24 \text{ cm s}^{-0.5}$ ) as the values of  $a$  for the Fine, and Coarse, heated reference soil (Table 2); but the values of the decay parameter  $b$  were about twice as large as those for the heated reference soils (Fig. 3, Table 2). Difference in sorptivity for dry soil moisture contents ( $< 0.02 \text{ cm}^3 \text{ cm}^{-3}$ ) were less significant ( $p = 0.11$ , two-tailed t-test) than for the heated reference soils. For Fine ash, the 1-D sorptivity measurements were significantly ( $p = 0.03$ ) less than the 3-D sorptivity measurements and had a poor fit to the exponential function ( $R^2 = 0.20$ , Table 2). The  $S$ - $\theta$  relation for ash appears to depend on particle size for  $\theta_i < 0.20 \text{ cm}^3 \text{ cm}^{-3}$ , but it is essentially independent of particle size for  $\theta_i > 0.20 \text{ cm}^3 \text{ cm}^{-3}$  (Fig. 3).

Values of  $S$  for fire-affected soil samples (with mixed grain sizes) were lower than those for the Fine, heated reference soils. For the Harvard soil, the few values of  $S$  (corresponding to dry con-

dition) were the lowest values of all samples, ranging from  $0.0003$  to  $0.013 \text{ cm s}^{-0.5}$  (mean =  $0.0065 \text{ cm s}^{-0.5}$ ) and were associated with the largest values of the water-repelleny metric ( $T_1 = 72 \text{ s}$  at  $0.012 \text{ cm}^3 \text{ cm}^{-3}$ ). Burned-field samples of Overland soil appear to have greater sorptivity than the Harvard soil (Fig. 4A), ranging from  $0.041$  to  $0.12 \text{ cm s}^{-0.5}$  (mean =  $0.070 \text{ cm s}^{-0.5}$ ) and a corresponding lower water-repelleny metric ( $T_1 = 4.9 \text{ s}$  at  $0.020 \text{ cm}^3 \text{ cm}^{-3}$ ); however, fewer measurements (see Table 2) and the large variance gives only a  $p$ -value =  $0.11$ .

Sorptivities of the Harvard soil (Burned-lab), measured at soil moisture content similar to those in the field ( $\sim 0.010 \text{ cm}^3 \text{ cm}^{-3}$ ), were greater ( $p = 0.0004$ ) than the Burned-field measurements. Average sorptivity was  $0.076 \text{ cm s}^{-0.5}$  for the 3-D measurements and  $0.049 \text{ cm s}^{-0.5}$  for the 1-D measurements (Fig. 4A). These sorptivities were about an order of magnitude greater than the field measurements ( $\sim 0.01 \text{ cm s}^{-0.5}$ ), and the corresponding water-repelleny metric was about an order of magnitude lower than the field measurement (Table 2). Laboratory measurements of  $S$  best-fit Eq. (10) with  $a = 0.11$  and  $0.078 \text{ cm s}^{-0.5}$  (3-D and 1-D, respectively) and had a relatively rapid decay constants of  $b = 16.3$  and  $22.5$  (Fig. 4A, Table 2).

Sorptivity relations for the Hi Meadow soil (Burned-lab) were similar to the Harvard soil (Burned-lab) at low soil moisture content (see values of  $a$  in Table 2). However, sorptivity relation for the Hi Meadow soil (Unburned-lab) was essentially constant, and thus, independent of initial soil moisture content. Moreover,  $S$  for the Unburned-lab was significantly ( $p = 0.01$ ) less than the sorptivity for the Burned-lab, and had correspondingly larger values of the water-repelleny metric (Fig. 4B, Table 2).

**Hydraulic conductivity**

Some field and laboratory measurements of  $K_f$  using the Mini-disk infiltrometer produced negative values when fit to Eqs. (2), (4), (5). Negative values (see “Discussion” below) of  $K_f$  were calculated for 3-D and 1-D measurements and were clustered at values of low soil moisture content where 79% corresponded to  $\theta_i/\theta_f \leq 0.10$ , and only 16% corresponded to  $\theta_i/\theta_f \geq 0.78$  near satu-

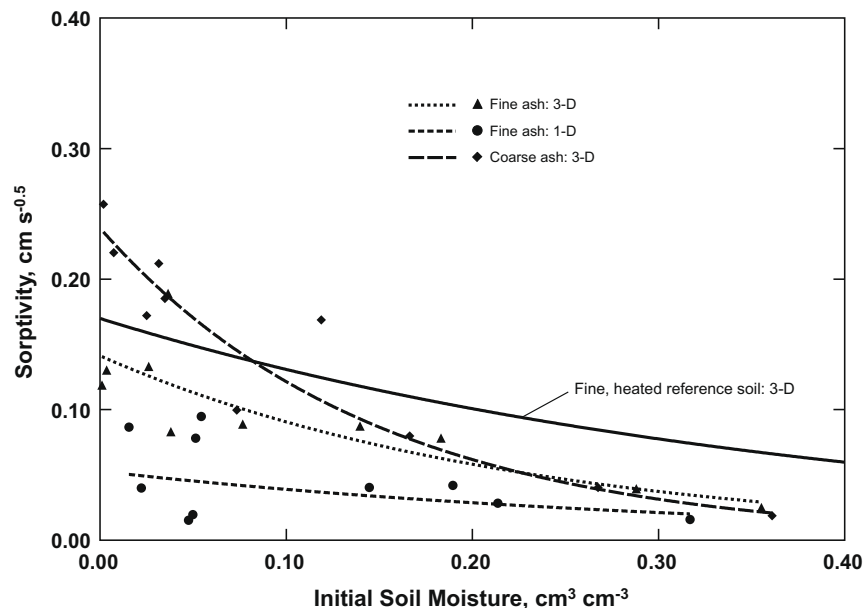


**Fig. 3.** Sorptivity as function of initial soil moisture content for one- and three-dimensional (1-D and 3-D) infiltrometer measurements and for two size classes of ash – Fine ash and Coarse ash. The empirical curve for the Fine, heated reference soil ( $< 0.063 \text{ mm}$ ; 3-D in Fig. 2A) is shown as a heavy line for comparison.

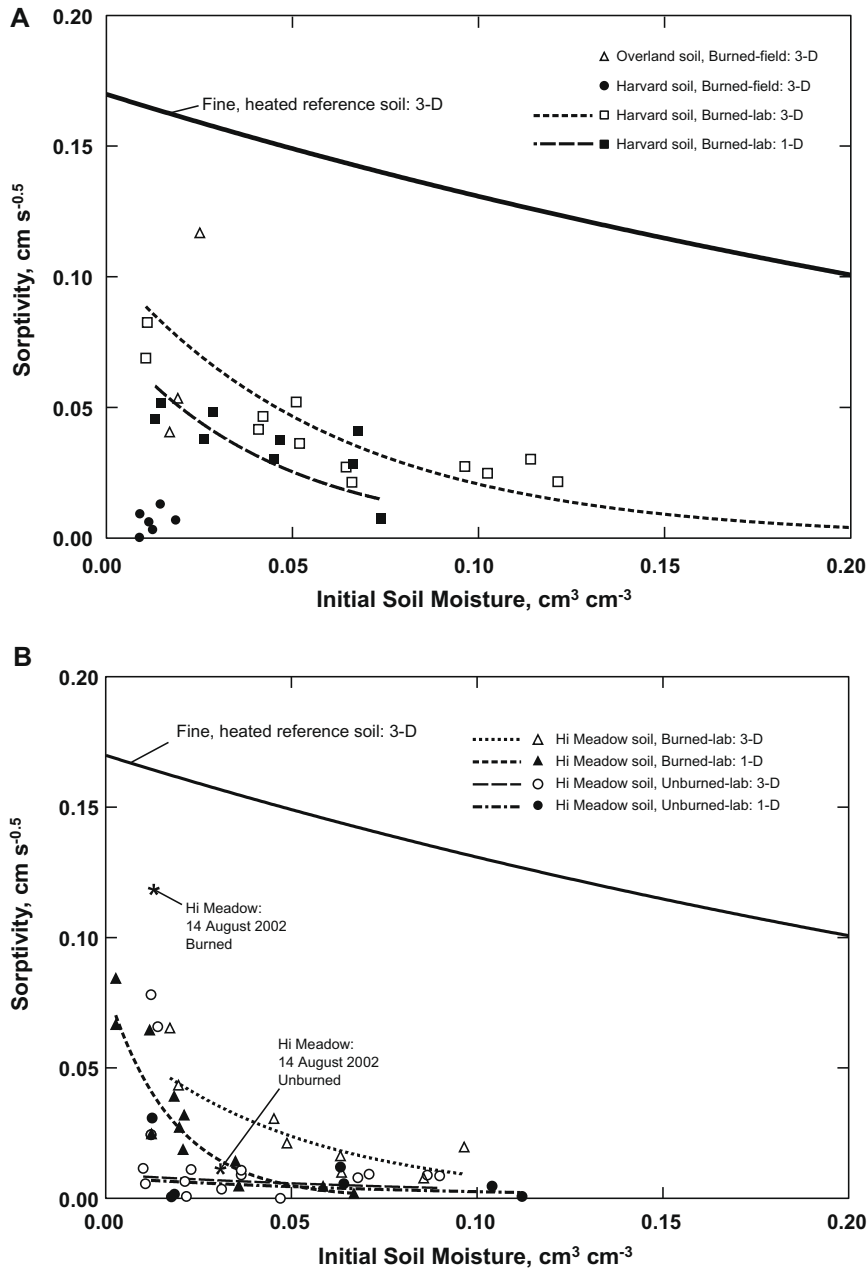


**Fig. 4.** Sorptivity as function of initial soil moisture content for soils from burned sites. Note the change in vertical scale relative to Figs. 2 and 3. The empirical curve for the fine, heated reference soil (<0.063 mm; 3-D in Fig. 2A) is shown as a heavy line for comparison. (A) Overland soil and Harvard soil. (B) Hi Meadow soil from burned area and unburned area adjacent to the Hi Meadow Fire.

ration. Negative values were small, ranging from  $-0.049$  to  $-0.00009$  cm s<sup>-1</sup> for reference soils and ash, from  $-0.012$  to  $-0.00019$  cm s<sup>-1</sup> for samples collected in the field (but measured in the laboratory), and  $-0.021$  to  $-0.0003$  cm s<sup>-1</sup> for measurements made in the field.

For reference soils, the dependence of  $K_f$  on particle size was unclear from the 1-D measurements, but  $K_f$  was dependent on water repellency (Table 2). Values of  $K_f$  for the natural reference soil were significantly less than  $K_f$  for the heated reference soils ( $p = 4 \times 10^{-7}$  for Fine, and  $p = 0.03$  for the Coarse, heated reference soil). Specifically,  $K_f$  for the Fine, natural reference soil (water repellent metric  $T_I = 4.2$  s) was about 5-fold less than  $K_f$  for Fine, heated reference soils ( $T_I = 2.4$  s), and  $K_f$  for the Coarse, natural reference soil ( $T_I = 2.5$  s) was only about 2-fold less than  $K_f$  for the Coarse, heated reference soil ( $T_I = 2.0$  s). (Table 2).

For ash, the mean of  $K_f$  ( $4.5 \times 10^3$  cm s<sup>-1</sup>, 1-D measurements) was essentially the same as the mean for both size classes of the reference soil considering the standard error of the measurements (Table 2). However, the 3-D mean value of  $K_f$  was about one order of magnitude greater than the 1-D value.

Individual field measurements in the Harvard Fire ranged from 0.0006 to 0.0019 cm s<sup>-1</sup> and the three field measurements in the Overland Fire site yielded small negative values ( $-0.00032$ ,  $-0.0040$ , and  $-0.021$  cm s<sup>-1</sup>; see "Discussion" below). For the Harvard soil (Burned-lab), the mean of the 3-D measurements was about six times greater ( $p = 0.0003$ ) than the mean of the 1-D measurements, even though the water-repellency metrics were similar (Table 2). Mean values of  $K_f$  for the Hi Meadow, Burned-lab and Unburned-lab soils were similar for 3-D and 1-D measurements ranging from  $0.86 \times 10^{-3}$  to  $3.0 \times 10^{-3}$  cm s<sup>-1</sup> (Table 2).



## Discussion

### Assessment of methodology

The difference between the 3-D and 1-D infiltration equations is the lateral capillary component of sorptivity. If Eq. (2) ( $I_{1D}$ ) is subtracted from Eq. (4) ( $I_{3D}$ ), then the plot of  $I_{3D}-I_{1D}$  versus time should be linear and the slope equal to  $\frac{\gamma S^2}{r_a(\theta_f-\theta_i)}$ . From this slope the proportionality constant,  $\gamma$ , which corrects for 3-D effects (Haverkamp et al., 1994), can be calculated. We used best-fit equations for 1-D and 3-D infiltration to estimate cumulative infiltration at 60-s intervals and then subtracted the 1-D from the 3-D estimates. Based on three similar sets of 1-D and 3-D measurements (Fine, heated reference soil for  $\theta_i = 0.0024, 0.012, \text{ and } 0.646 \text{ cm}^3 \text{ cm}^{-3}$ ) the difference  $I_{3D}-I_{1D}$  gave estimates of  $\gamma$  ranging from 0.7 to 1.1. These values of  $\gamma$  for the Fine, heated reference soil tend to be greater than those (0.6–0.8) reported by Haverkamp et al. (1994) and the essentially constant values (0.704–0.750) reported by Smettem et al. (1995). These last values are for Redlands sandy loam (Oxic Paleustalf), which would have some natural water repellency. Our values of  $\gamma$  are for heated reference soils with a low value of the water-repellency metric ( $T_1 = 1.1 \text{ s}$ ). The difference suggests that  $\gamma$  is greater for soils with low degree of water repellency, or in other words,  $\gamma$  may be reduced by water-repellent compounds common in many soils.

Values of hydraulic conductivity and sorptivity should not depend on the measurement method. However, 3-D measurements for the mean  $K_f$  ranged from  $\sim 2.5$  times (Fine ash) to 30 times (Coarse, heated reference soil) greater than the 1-D measurements (Table 2). Comparing Eqs. (7) and (8) indicates that the 3-D value of  $K_f$  would be less if  $\gamma$  were larger, which supports using the larger values of  $\gamma$  estimated above. Sorptivities for the different types of materials, calculated using the 3-D measurements, were similar at low soil moisture content (compare values of  $a$  in Table 2), but generally the decay constant  $b$  was smaller for the 3-D measurements than the 1-D measurements. This lower sorptivity for the 1-D measurements may reflect the restricted lateral flow that was intentionally designed to satisfy the assumptions of 1-D infiltration; however, this may limit the use of 1-D measurements for sorptivity. The conundrum is that most models of infiltration use the 1-D simplification. However, we speculate at this point, based on some field and laboratory observations, that initial infiltration from raindrops may be 3-D such that the drops spread laterally and only after a period of time will the drops “connect” and form a thin layer that could be modeled as 1-D infiltration. This conceptual model seems to be supported by our result for ash, where the sorptivity appears to depend on particle size for  $\theta_i < 0.20 \text{ cm}^3 \text{ cm}^{-3}$ , but is essentially independent of particle size for  $\theta_i > 0.20 \text{ cm}^3 \text{ cm}^{-3}$  (Fig. 3) when connection of pore spaces between particles would be more common and form a thin, connected layer of water.

A few negative values of  $K_f$  were calculated, which are obviously not physical. Most were associated with low initial soil moisture content. Repeated wetting and drying of the soil samples in the laboratory may have altered the water repellency causing some of the observed variability in  $K_f$  at low soil moisture content. The most likely explanations for the negative values are probably measurement error or the mathematical approximations used to derive the infiltration equation. Although the infiltration volumes were accurate to  $\pm 0.5 \text{ mL}$  and the time resolution was  $0.01 \text{ s}$ , the accuracy of the time was dependent on a visual determination of the infiltrated volume by reading the graduated scale on the Mini-disk infiltrometer. Measurement error was largest when infiltration was the most rapid at low soil moisture content. The second explanation also relates to low soil moisture content. The gravity term in Eq. (4), at early times, may be more significant at low soil moisture

content than the vertical or lateral capillary terms. Derivation of infiltration Eq. (4) assumes that sorptivity dominates at early times, and thus by including only sorptivity, the sorptivity term would be over estimated and negative values of  $K_f$  would be required to balance the infiltration flux (per comm. Markus Berli, 2008). This may indicate that the proportionality constant,  $\gamma$ , may differ from the accepted values as suggested above or that the infiltration equation needs to be reformulated for application to dry soils.

### Sorptivity and hydraulic conductivity values for modeling

The magnitude of the sorptivity measured with the Mini-disk infiltrometer yielded reasonable values compared to some published values. For example, the average sorptivity for dry sand with uniform particle size ( $\theta_i = 0.009 \text{ cm}^3 \text{ cm}^{-3}$ ; median diameter =  $0.15 \text{ mm}$ ) was  $0.212 \text{ cm s}^{-0.5}$  (Culligan et al., 2005), which is in the range of values near zero for the Coarse, heated reference soil ( $0.20$  and  $0.23 \text{ cm s}^{-0.5}$ ,  $a$  in Table 2). Other soils did not have uniform particle size, but were similar in texture. Sorptivity was  $0.12 \text{ cm s}^{-0.5}$  for loamy-sand and sandy-loam soils (Smith, 1999; no values of soil moisture content were given), and it was  $0.058$ – $0.105 \text{ cm s}^{-0.5}$  ( $\theta_i = 0.02 \text{ cm}^3 \text{ cm}^{-3}$ ; Wang et al., 2006) for silty soils. The form of the  $S$ – $\theta$  was similar to existing exponential forms (Parlange, 1975; Kutilek and Valentová, 1986; Lockington, 1993; Wang et al., 2006). Values of  $a$  (in Eq. (10), see Table 2) were similar to the value of  $a = 0.245 \text{ cm s}^{-0.5}$  selected by Kutilek and Valentová (1986). Thus, it appears that the Mini-disk infiltrometer can be used to measure  $S$  and provide estimates of  $K_f$ , which can be used in physically-based, rainfall–infiltration–runoff models of fire-affected soils.

Field and laboratory values of  $K_f$  for fire-affected soils were within a relatively narrow range from  $0.86 \times 10^{-3} \text{ cm s}^{-1}$  to  $7.7 \times 10^{-3} \text{ cm s}^{-1}$ . In contrast, values of  $K_{sat}$  published in the literature can range over 2–4 orders of magnitude for sand- and clay-size material (Hillel, 1998). Values of  $K_f$  overlapped other steady infiltration rates (which should approach  $K_{sat}$  at longer times) measured on fire-affected soils ( $0.28 \times 10^{-3}$ – $2.8 \times 10^{-3} \text{ cm s}^{-1}$ ; Kinner and Moody, 2008; Martin and Moody, 2001). Some of the higher values of  $K_f$  in this study may be related to repacking the soil before each measurement in the laboratory, which can never replicate in situ soils. Soils from the burned areas were Coarser and more difficult to repack than the reference soils, which had a standard error in the value of the bulk density of 2.5% for Fine, and 1.5% for Coarse, heated reference soils (Table 1). Six in situ field measurements in the Harvard Fire site, ranged from  $0.56 \times 10^{-3}$  to  $1.9 \times 10^{-3} \text{ cm s}^{-1}$ . This range is similar to ranges based on rainfall simulations:  $0.69 \times 10^{-3}$ – $1.4 \times 10^{-3} \text{ cm s}^{-1}$  for burned Mediterranean scrubland (Cerdà, 1998),  $0.28 \times 10^{-3}$ – $2.5 \times 10^{-3} \text{ cm s}^{-1}$  after prescribed fire (Robichaud, 2000), and  $1.3 \times 10^{-3}$ – $2.0 \times 10^{-3} \text{ cm s}^{-1}$  in burned steep rangeland (Pierson et al., 2001). Thus, the Mini-disk also provides reliable, in situ, field measurements of  $K_f$  for modeling purposes.

Models of infiltration and runoff from burned watersheds need to address the physics of a two-layer system consisting of ash on top of mineral soil. Our results provide the first measurements of the  $S$  and  $K_f$  for ash. Mean  $K_f$  and  $S$ – $\theta$  relation for ash were similar to those for heated reference soil (Figs. 2 and 3; Table 2), but greater than those for the fire-affected soil (Hi Meadow and Harvard soils). Infiltration into ash appears to be controlled by sorptivity (see “Discussion” below where sorptivity terms are  $\sim 1$ – $5$  times  $>$ hydraulic conductivity terms, Table 3). Ash has a relatively large capacity to store water ( $0.90 \text{ g water per } 1 \text{ g of ash}$  or  $0.61 \text{ cm}^3 \text{ cm}^{-3}$ ; standard error =  $\pm 2\%$ ), and thus, acts as a hydrophilic layer (Doerr et al., 2000). Water stored initially in the ash, either runs off as saturated overland flow or moves laterally down-

**Table 3**  
Ratio of sorptivity terms to hydraulic conductivity terms for selected soil samples.

Elapsed time (min)	Fine, natural reference soil, 1-D initial soil moisture values ( $\text{cm}^3 \text{cm}^{-3}$ )			Harvard soil, 3-D initial soil moisture values ( $\text{cm}^3 \text{cm}^{-3}$ )		Fine ash, 3-D initial soil moisture values ( $\text{cm}^3 \text{cm}^{-3}$ )	
	0.02	0.10	0.20	0.02	0.10	0.02	0.10
1	24.8	12	4.8	4.9	1.00	4.8	3.1
10	7.8	3.8	1.5	2.9	0.44	2.8	1.7
20	5.5	2.7	1.1	2.6	0.37	2.5	1.5
30	4.5	2.2	0.88	2.5	0.34	2.4	1.4
60	3.2	1.5	0.62	2.3	0.29	2.2	1.3

slope as throughflow above the fire-affected soil (Kinner and Moody, in review, J. Hydrology).

#### Linking water repellency to hydraulic properties

Sorptivity and hydraulic conductivity are inversely linked to the degree of water repellency. Metrics used to indicate the degree of water repellency (molarity of ethanol droplets, MED, Letey et al., 1962, 2000; King, 1981; and critical surface tension, CST, Huffman et al., 2001) can be related to  $S$  and  $K_f$  (Philip, 1954). However, these water-repellency metrics cannot be used directly in predictive rainfall–infiltration–runoff models, whereas  $S$ – $\theta$  relations and  $K_f$  can. At low soil moisture content, water repellency limits the wetting of some grains thereby reducing the capillary suction or capillary potential in some pores. If the capillary potential decreases then  $S$  decreases, and if some pores are not active, then water flows through fewer pores, and  $K_f$  decreases. Sorptivity and hydraulic conductivity for the natural reference soils were about two and five times less than the values for heated reference soils (Fig. 2, Table 2), indicating that the heating to 550 °C did remove some, or all, of the water-repellent compounds, and thus, decreased the water repellency. This result agrees with other work by Nakaya et al. (1977) who showed that heating soil to 250 °C increases the capillary suction (i.e. decreases the water repellency) relative to soils heated to only 105 °C. Measurements of  $S$  and  $K_f$  indicate that the natural reference soils were more water repellent than the heated reference soils over a wide range of values of initial soil moisture content, whereas the water-repellency metrics such as,  $T_1$ , WDPT, CST, and MED only provide estimates at a specific soil moisture content and in the case of  $T_1$  only suggests a slight increase in water repellency (Table 2).

The dominance of sorptivity and hydraulic conductivity in controlling infiltration will change with time during a rainstorm and these changes will depend on  $\theta_i$ . To investigate this change with time, the ratio of the sorptivity terms to hydraulic conductivity terms in Eqs. (2) and (5) was computed using the hydraulic relations in Table 2 for 60 min, which is a typical duration for orographic convective storms (Hershfield, 1961; Moody and Martin, 2001; Moody et al., 2007a). Eq. (2) has one sorptivity term (vertical capillarity) and one hydraulic conductivity term, whereas Eq. (5) has two sorptivity terms (vertical and lateral capillarity), but still one hydraulic conductivity term. All the ratios decreased with elapsed time indicating that sorptivity was most dominant for early times and hydraulic conductivity became more dominant as time elapsed (Table 3). The ratio also decreased with increase in the initial soil moisture content. For the Fine, natural reference soil and  $\theta_i = 0.20 \text{ cm}^3 \text{ cm}^{-3}$ , the ratio decreased below 1.0 at 26 min indicating the  $K_f$ -terms were greater than the  $S$ -terms. This happened much sooner ( $\sim 1.1$  min) for the Harvard soil with a drier initial soil moisture content ( $0.10 \text{ cm}^3 \text{ cm}^{-3}$ , Table 3). In all cases, as  $\theta_i$  approaches saturation, water repellency is probably no longer affected by sorptivity and hydraulic conductivity because water repellency essentially disappears, not because of physical process,

but because of a change in the chemical property of the molecules of water-repellent compound (Doerr et al., 2000).

#### Extremely dry soil conditions

Extremely dry soil conditions, in this paper, are defined as the domain where  $\theta_i < 0.02 \text{ cm}^3 \text{ cm}^{-3}$ . Heat from wildfires probably drives off more adsorbed water from the surface of soil particles and soil aggregates than does the heat during drought conditions. Re-adsorption during the first rain after a wildfire is probably the first process in rewetting the soil. This process takes time during which little water can infiltrate until the capillary pressure is re-established, and consequently more of the rainfall must be transformed into increased runoff. Sometimes this rewetting process has been referred to as “film flow” (McQueen and Miller, 1968; Hillel, 1998, Chapter 6; Bachmann and van der Ploeg, 2002; Tuller and Or, 2002). This process contrasts with capillary and gravity processes operating in connected pores spaces between soil particles and aggregates.

Extremely dry soil conditions during a drought can be maintained longer under a litter and duff layer in unburned area than in a burned area without litter and duff. Measurements made during a drought in 2002 in the Hi Meadow Fire site (see asterisks in Fig. 4B) showed that the water-repellency metric,  $T_1$  (41 s) in the unburned area was greater than  $T_1$  (2.7 s) in the burned area (Table 2). Soil from the unburned area had more organic material than soil from the burned area (Table 1), and this organic material probably was partially responsible for the increase in the degree of water repellency (Doerr et al., 2000). Measurements showed that  $S$  (essential constant  $\sim 0.010$ – $0.016 \text{ cm s}^{-0.5}$ ) for the Hi Meadow (Unburned-lab) soil was less than  $S$  for Hi Meadow (Burned-lab) soils (see curves in Fig. 4B). Values of  $K_f$  for the soils from the two areas were essentially the same, within the measurement error. Therefore, it was the values of the sorptivity, in this situation, that indicate the soil from the unburned area was more water repellent than the soil from the burned area. Data collected during a drought in 2002, verified increased runoff during dry soil conditions when  $\theta_i$  ranged from 0.023 to  $0.057 \text{ cm}^3 \text{ cm}^{-3}$  (Moody et al., 2007b). Runoff during a rainstorm from the unburned area ( $0.64 \text{ L m}^{-2}$  per mm of rain) was actually greater than the runoff during the same storm from the adjacent burned area ( $0.27 \text{ L m}^{-2}$  per mm of rain; unpublished data for 29 August 2002, J. Moody and D. Martin). During wetter conditions this was not observed to be the case.

#### Sorptivity maximum

Examining more closely the  $S$ – $\theta$  relation in the extremely dry domain suggests a sorptivity maximum with sorptivity decreasing as the soil moisture approaches saturation and as it approaches zero. This maximum appears between 0.02 and  $0.08 \text{ cm}^3 \text{ cm}^{-3}$  for the Fine, heated reference soil (Fig. 5). Perhaps, yet less defined, between  $\theta_i = 0.02$  and  $0.04 \text{ cm}^3 \text{ cm}^{-3}$  for the Coarse, heated reference soil and even better defined if a few points (enclosed in ellip-

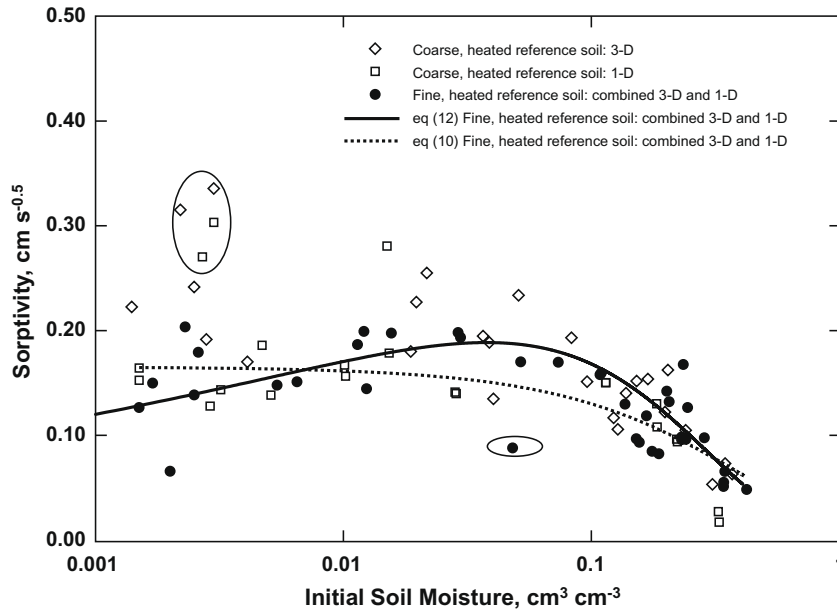


Fig. 5. Details of the sorptivity–soil moisture relation in the extremely dry domain where values of soil moisture content are typically  $<0.02 \text{ cm}^3 \text{ cm}^{-3}$ . Points enclosed in ellipses indicate possible outliers.

ses in Fig. 5) are considered as possible outliers. A higher degree of water repellency (i.e. a lower sorptivity as soil moisture approaches zero) in Fine soils also was reported de Jonge et al. (1999). This non-linear behavior (a maximum in sorptivity) in this domain may reflect a transition between the capillary process and adsorption processes. A similar non-linear behavior of water repellency has been observed by others in this domain (King, 1981; Nakaya et al., 1977; de Jonge et al., 1999; Blonquist et al., 2006; Leelamanie and Karube, 2007; Regalado et al., 2008). However, sorptivity in this domain must be considered as an “equivalent sorptivity” resulting from extrapolating Eqs. (2) and (5), which describe capillary and gravity processes, into this transitional domain that includes a combination of capillary, gravity, and adsorption processes.

An empirical equation for sorptivity was developed that incorporated a possible maximum in sorptivity within the extremely dry soil domain. Existing analytical formulations approximate the sorptivity relation by

$$S^2 = 2(\theta_s - \theta_i) \int_{\theta_i}^{\theta_s} D(\theta) d\theta, \quad (11)$$

where  $\theta_s$  is the saturated soil moisture content [ $\text{L}^3 \text{ L}^{-3}$ ], and  $D(\theta)$ , is the soil diffusivity, [ $\text{LT}^{-2}$ ] (Parlange, 1975; Parlange et al., 1985; Haverkamp et al., 1994). Parlange (1975) has suggested that  $D(\theta)$  might have the form of  $D_0 e^{B\theta}$  or  $D_0 \theta^B$ , ( $D_0$  and  $B$  being constants), which has been investigated by others (Kutílek and Valentová, 1986; Wang et al., 2006). All these forms produce a monotonically decreasing, non-linear function for the  $S$ – $\theta$  relation starting as some constant at  $\theta_i = 0$  and approaching zero as  $\theta_i \rightarrow \theta_s$ , and therefore, will not represent a possible sorptivity maximum. We therefore fit a modified form of Eq. (10) given by

$$S = \theta_i^c a' e^{-b'\theta_i} \quad (12)$$

such that  $S$  approaches zero as  $\theta_i \rightarrow 0$ , and also, as  $\theta_i \rightarrow \theta_s$  allowing for a maximum value of sorptivity.

We combined the 3-D and 1-D measurements for the Fine, heated reference soil to provide sufficient data to statistically resolve this equation for sorptivity in the extremely dry domain. The goodness-of-fit metric,  $R^2$ , for this modified form (Eq. (12) with

$c = 0.169$ ,  $a' = 0.385$ , and  $b' = 5.0$ ) was 0.52, and has a sorptivity maximum of  $0.18\text{--}0.20 \text{ cm s}^{-0.5}$  between  $0.03$  and  $0.08 \text{ cm}^3 \text{ cm}^{-3}$  (Fig. 5). For Fine ash, with fewer data, the sorptivity maximum was less well defined between  $0.03$  and  $0.04 \text{ cm}^3 \text{ cm}^{-3}$  using the modified sorptivity equation ( $R^2 = 0.50$ ). Fire-affected soils did not have sufficient measurements for  $\theta_i < 0.01 \text{ cm}^3 \text{ cm}^{-3}$  to resolve the possible sorptivity maximum. This modified form of the  $S$ – $\theta$  relation for the Fine, heated reference soil represents  $S$  as well as the exponential form for the combined 1-D and 3-D data (Eq. (10):  $a = 0.165$ ,  $b = 2.4$ ;  $R^2 = 0.53$ ). These results suggest a possible non-linear behavior characterized by a sorptivity maximum. The sorptivity maximum indicates that there would be a corresponding critical soil moisture content such that the sorptivity decreases above and below this value. Sorptivity below this critical value probably should be referred to as “equivalent sorptivity” because this is a transitional domain, which includes a combination of capillary, gravity, and adsorption processes.

Many investigators have measured such a critical soil-moisture threshold below which moderate to extreme water repellency is measured. For example, measurements made by Dekker et al. (2001) near the surface of dunes sands indicate a threshold at  $\sim 0.18 \text{ cm}^3 \text{ cm}^{-3}$ , which decreases to  $0.05$  and  $0.02 \text{ cm}^3 \text{ cm}^{-3}$  at depths of  $0.14$  and  $0.19 \text{ m}$ , and MacDonald and Huffman (2004) estimated the threshold to be  $\sim 0.10$  and  $0.26 \text{ cm}^3 \text{ cm}^{-3}$  for soils in unburned and burned areas. Values of soil moisture content greater than those for the Fine, heated reference soil may reflect the water repellency of natural soils. This critical soil-moisture threshold may correspond to the values of the soil moisture content at the sorptivity maximum predicted by Eq. (12).

### Summary and conclusions

This research was motivated by the possibility that wildfires can produce extremely dry conditions in the upper layer of the soil, and thus, change the soil physics controlling runoff in burned watersheds. We used a portable infiltrometer to measure the near-saturated hydraulic conductivity,  $K_f$ , and the sorptivity–soil moisture relation,  $S(\theta_i, \theta_f)$ , over a range of values of the initial soil moisture content that include the extremely dry domain

( $\theta_i < 0.02 \text{ cm}^3 \text{ cm}^{-3}$ ) to near saturation. Cumulative infiltration was measured in the field and in the laboratory for reference soils, ash, soil unaffected by fire, and fire-affected soils under 3-D conditions and conditions approximating 1-D infiltration. The value of the parameter  $\gamma$ , used to correct for 1-D approximation, was found to be greater (0.7–1.1) than the published values (0.7–0.8) suggesting that  $\gamma$  may depend on the degree of water repellency.

We found that  $K_f$  was inversely related to the degree of water repellency. The range of  $K_f$  was largest ( $3.8 \times 10^{-3}$ – $130 \times 10^{-3} \text{ cm s}^{-1}$ ) for the heated reference soils with a low water-repellency metric ( $0.4 \text{ s} < T_1 < 2.4 \text{ s}$ ), lower for the fire-affected soils ( $1.1 \times 10^{-3}$ – $7.7 \times 10^{-3} \text{ cm s}^{-1}$ ;  $5.6 \text{ s} < T_1 < 72 \text{ s}$ ), and surprisingly lowest for soil from an unburned area ( $0.86 \times 10^{-3}$ – $3.0 \times 10^{-3} \text{ cm s}^{-1}$ ;  $16 \text{ s} < T_1 < 41 \text{ s}$ ). Ash also had relatively large values of  $K_f$ , ranging from  $4.5 \times 10^{-3}$ – $53 \times 10^{-3} \text{ cm s}^{-1}$  with relatively low values of the water-repellency metric ( $0.6 \text{ s} < T_1 < 3.6 \text{ s}$ ).

Similarly,  $S$  was inversely related to the degree of water repellency. For the Fine, heated reference soil and for Fine ash, we identified a sorptivity maximum of  $0.18$ – $0.20 \text{ cm s}^{-0.5}$  in the extremely dry domain ( $0.03 < \theta_i < 0.08 \text{ cm}^3 \text{ cm}^{-3}$ ). This non-linear dependence on  $\theta_i$  may explain the observed non-linear behavior of water repellency and the critical soil-moisture threshold associated with water repellent soils. Above this critical soil moisture content corresponding to the sorptivity maximum, sorptivity decreases but hydraulic conductivity is essentially constant such that the water repellency will depend on the relative importance of sorptivity and hydraulic conductivity in each specific soil. Below this critical soil-moisture threshold is a transitional domain that includes a combination of capillary, gravity, and adsorption processes. Here the “equivalent sorptivity” decreases reflecting the corresponding observed increase in water repellency.

These empirical  $S$ – $\theta$  relations are valuable because they contain the essential soil moisture dependence of sorptivity and consequently water repellency. Water-repellency metrics such as  $T_1$ , WDPT, CST, and MED do not have the necessary soil moisture-dependent information. Our results also provide the first measurements of  $K_f$  and  $S$  for ash, which must be included in a two-layer model. These relations, especially for the extremely dry domain, are compatible with, and therefore, can be used in physically-based models to predict runoff for the initial conditions after a wildfire.

## Acknowledgments

We want to thank Wahad Sadeqi for the careful and sometimes tedious preparation procedures for the reference soils. Discussions with Dr. Roger Smith were fruitful in making the 1-D measurements as well as steering us through the theory. Review comments and suggestions by Jonathan Godt (US Geological Survey, Golden, Colorado), Markus Berli (Desert Research Institute, University of Nevada, Nevada), John Nimmo (US Geological Survey, Menlo Park, California), Juan Giraldez (Associate Editor), and three anonymous reviewers helped to clarify several topics and to make definite improvements in the content and organization of the paper.

Any use of trade, firm, or product names is for descriptive purposes only and does not imply endorsement by the US Government.

## References

Bachmann, J., van der Ploeg, R.R., 2002. A review on recent developments in soil water retention theory: interfacial tension and temperature effects. *J. Plant Nutr. Soil Sci.* 165, 468–478.

Bauters, T.W.J., Steenhuis, T.S., DiCarlo, D.A., Nieber, J.L., Dekker, L.W., Ritsema, C.J., Parlange, J.-Y., Haverkamp, R., 2000. Physics of water repellent soils. *J. Hydrol.* 231–232, 233–243.

Blonquist, J.M.Jr., Jones, S.B., Lebron, L., Robinson, D.A., 2006. Microstructural and phase configurational effects determining water content: Dielectric

relationships of aggregated porous media. *Water Resour. Res.* 42, Wo5424. doi:10.1029/2005WR004418.

Brooks, R.H., Corey, A.T., 1964. Hydraulic properties of porous media, *Hydrol. Paper 3*, Civil Engineering Department, Colorado State University, Fort Collins, 27 p.

Cerdà, A., 1998. Changes in overland flow and infiltration after a rangeland fire in a Mediterranean scrubland. *Hydrol. Process.* 12, 1031–1042.

Culligan, P.J., Ivanov, V., Germaine, J.T., 2005. Sorptivity and liquid infiltration into dry soil. *Adv. Water Resour.* 28, 1010–1020.

Czachor, H., 2006. Modelling the effect of pore structure and wetting angles on capillary rise in soils having different wettabilities. *J. Hydrol.* 328, 604–613.

de Jonge, L.W., Jacobsen, O.H., Moldrup, P., 1999. Soil water repellency: effects of water content, temperature, and particle size. *Soil Sci. Soc. Am. J.* 63, 437–442.

DeBano, L.F., 2000. The role of fire and soil heating on water repellency in wildland environments: a review. *J. Hydrol.* 231–232, 195–206.

Decagon, 2006. Mini Disk Infiltrometers User's Manual, Decagon Devices. Pullman, WA. 18 p.

Dekker, L.W., Doerr, S.H., Oostindie, K., Ziogas, A.K., Ritsema, C.J., 2001. Water repellency and critical soil water content in a dune sand. *Soil Sci. Soc. Am. J.* 65, 1667–1674.

Doerr, S.H., 1998. On standardizing the ‘Water drop penetration time’ and the ‘Molarity of an ethanol droplet’ techniques to classify soil hydrophobicity: a case study using medium textured soils. *Earth Surf. Process. Land.* 23, 663–668.

Doerr, S.H., Shakesby, R.A., Walsh, R.P.D., 2000. Soil water repellency: its causes, characteristics and hydro-geomorphological significance. *Earth-Sci. Rev.* 51, 33–65.

Fox, D.M., Darboux, F., Carrega, P., 2007. Effects of fire-induced water repellency on soil aggregate stability, splash erosion, and saturated hydraulic conductivity for different size fractions. *Hydrol. Process.* 21, 2377–2384.

Green, W.H., Ampt, G.A., 1911. Studies on soil physics, part I. The flow of air and water through soils. *J. Agri. Sci.* 4, 1–24.

Haverkamp, R., Ross, P.J., Smettem, K.R.J., Parlange, J.Y., 1994. Three-dimensional analysis of infiltration from the disc infiltrometer 2. Physically based infiltration equation. *Water Resour. Res.* 30 (11), 2931–2935.

Hershfield, D.M., 1961. Rainfall frequency atlas of the United States for duration from 30 minutes to 24 hours and return periods from 1 to 100 years. US Department of Commerce.

Hillel, D., 1998. *Environmental Soil Physics*. Academic Press, New York.

Huffman, E.L., MacDonald, L.H., Stednick, J.D., 2001. Strength and persistence of fire-induced soil hydrophobicity under ponderosa and lodgepole pine, Colorado Front Range. *Hydrol. Process.* 15, 2877–2892.

Humphreys, F.R., Craig, F.G., 1981. Effects of fire on soil chemical, structural and hydrological properties. In: Gill, A.M. (Ed.), *Fire and The Australian Biota*. Australian Academy of Science, Canberra, Australia, pp. 177–200 (Chapter 8).

Johnson, E.A., Miyaniishi, K., 2001. *Forest Fires Behavior and Ecological Effects*. Academic Press, New York. 600 pp.

Jones, T.P., Chaloner, W.G., Kuhlbusch, T.A.J., 1997. Proposed bio-geological and chemical based terminology for fire-altered plant matter. In: Clark, J.S., Cachier, H., Goldammer, J.G., Stocks, B. (Eds.), *Sediment Records of Biomass Burning and Global Change*. Springer-Verlag, Berlin, pp. 9–22.

Khlosi, M., Cornelis, W.M., Douaik, A., van Genuchten, M.Th., Gabriels, D., 2008. Performance evaluation of models that describe the soil water retention curve between saturation and oven dryness. *Vadose Zone J.* 7, 87–96.

King, P.M., 1981. Comparison of methods for measuring severity of water repellence of sandy soils and assessment of some factors that affect its measurement. *Aust. J. Soil Res.* 19, 275–285.

Kinner, D.A., Moody, J.A., 2008. Infiltration and runoff measurements on steep burned hillslopes using a rainfall simulator with variable rain intensities. US Geological Survey Scientific Investigations Report 2007-5211, 64 p.

Kinner, D.A., Moody, J.A. in review. Examining steady flow in rainfall simulation experiments on burned plots. *Hydrol. Process.*

Kutílek, M., Valentová, J., 1986. Sorptivity approximations. *Transport Porous Med.* 1, 57–62.

Leelamanie, D.A.L., Karube, J., 2007. Effects of organic compounds, water content and clay on the water repellency of a model sandy soil. *Soil Sci. Plant Nutr.* 53, 711–719.

Letey, J., 2001. Causes and consequences of fire-induced soil water repellency. *Hydrol. Process.* 15, 2867–2875.

Letey, J., Osborn, J., Pelishek, R.E., 1962. Measurement of liquid–solid contact angles in soil and sand. *Soil Sci.* 93 (3), 149–153.

Letey, J., Carrillo, M.L.K., Pang, X.P., 2000. Approaches to characterize the degree of water repellency. *J. Hydrol.* 231–232, 61–65.

Lockington, D., 1993. Estimating the sorptivity for a wide range of diffusivity dependence on water content. *Transport Porous Med.* 10, 95–101.

MacDonald, L.H., Huffman, E.L., 2004. Post-fire soil water repellency: persistence and soil moisture thresholds. *Soil Sci. Soc. Am. J.* 68, 1729–1734.

Marshall, T.J., Holmes, J.W., Rose, C.W., 1996. *Soil Physics*. Cambridge University Press, New York. 453 p.

Martin, D.A., Moody, J.A., 2001. Comparison of soil infiltration rates in burned and unburned mountainous watersheds. *Hydrol. Process.* 15, 2893–2903.

Massman, W.J., Frank, J.M., Shepperd, W.D., Platten, M.J., 2003. In situ soil temperature and heat flux measurements during controlled surface burns at a southern Colorado forest site. In: *USDA Forest Service Proceedings RMRS-P-29*, pp. 67–85.

McQueen, I.S., Miller, R.F., 1968. Calibration and evaluation of a wide-range gravimetric method for measuring moisture stress. *Soil Sci.* 106 (3), 225–231.

- Moody, J.A., Martin, D.A., 2001. Post-fire, rainfall intensity-peak discharge relations for three mountainous watersheds in the western USA. *Hydrol. Process.* 15, 2981–2993.
- Moody, J.A., Martin, D.A., Haire, S.L., Kinner, D.A., 2007a. Linking runoff response to burn severity after wildfire. *Hydrol. Process.* 1, 1–10. doi:10.1002/hyp.6806.
- Moody, J.A., Martin, D.A., Oakley, T.M., Blanken, P.D., 2007b. Temporal and spatial variability of soil temperature and soil moisture after a wildfire. US Geological Survey Scientific Investigations Report 2007-5015, 89 p.
- Nakaya, N., Yokoi, H., Motomura, S., 1977. The method for measuring of water repellency of soil. *Soil Sci. Plant Nutr.* 23 (4), 417–426.
- Neary, D.G., Klopatek, C.C., DeBano, L.F., Ffolliott, P.F., 1999. Fire effects on belowground sustainability: a review and synthesis. *Forest Ecol. Manag.* 122, 51–71.
- Onda, Y., Dietrich, W.E., Booker, F., 2008. Evolution of overland flow after a severe forest fire, Point Reyes, California. *Catena* 72, 13–20.
- Parlange, J.-Y., 1975. On solving the flow equation in unsaturated soils by optimization: horizontal infiltration. *Soil Sci. Soc. Am. Proc.* 39, 415–418.
- Parlange, J.-Y., Haverkamp, R., Touma, J., 1985. Infiltration under ponded conditions: 1. Optimal analytical solution and comparison with experimental observations. *Soil Sci.* 139 (4), 305–311.
- Philip, J.R., 1954. An infiltration equation with physical significance. *Soil Sci.* 77, 153–157.
- Philip, J.R., 1957a. Theory of infiltration. In: Chow, V.T. (Ed.), *Advances in Hydrosience*, vol. 5. Academic Press, New York, pp. 215–296.
- Philip, J.R., 1957b. The theory of infiltration: 1. The infiltration equation and its solution. *Soil Sci.* 83, 345–357.
- Philip, J.R., 1957c. The theory of infiltration: 4. Sorptivity and algebraic infiltration equations. *Soil Sci.* 84, 257–264.
- Pierson, F.B., Robichaud, P.R., Spaeth, K.E., 2001. Spatial and temporal effects of wildfire on the hydrology of a steep rangeland watershed. *Hydrol. Process.* 15, 2905–2916.
- Regalado, C.M., Ritter, A., de Jonge, L.W., Kawamoto, K., Komatsu, T., Moldrup, P., 2008. Useful soil–water repellency indices: linear correlations. *Soil Sci.* 173 (11), 747–757.
- Robichaud, P.R., 2000. Fire effects on infiltration rates after prescribed fire in Northern Rocky Mountain forests, USA. *J. Hydrol.* 231–232, 220–229.
- Robichaud, P.R., Lewis, S.A., Ashmun, L.E., 2008. New procedure for sampling infiltration to assess post-fire soil water repellency. USDA, Forest Service, RMRS-RN-33, 14 p.
- Ryan, K.C., 2002. Dynamic interactions between forest structure and fire behavior in boreal ecosystems. *Silva Fenn.* 36 (1), 13–39.
- Shirtcliffe, N.J., McHale, G., Newton, M.I., Pyatt, F.B., Doerr, S.H., 2006. Critical conditions for the wetting of soils. *Appl. Phys. Lett.* 89, 094101-1–094101-3.
- Smettem, K.R.J., Parlange, J.Y., Ross, P.J., Haverkamp, R., 1994. Three-dimensional analysis of infiltration from the disc infiltrometer. 1. A capillary-based theory. *Water Resour. Res.* 30, 2925–2929.
- Smettem, K.R.J., Ross, P.J., Haverkamp, R., Parlange, J.Y., 1995. Three-dimensional analysis of infiltration from the disc infiltrometer. 3. Parameter estimation using a double-disk tension infiltrometer. *Water Resour. Res.* 31 (10), 2491–2495.
- Smith, R.E., 1990. Analysis of infiltration through a two-layer soil profile. *Soil Sci. Soc. Am. J.* 54, 1219–1227.
- Smith, R.E., 1999. Technical note: rapid measurement of soil sorptivity. *Soil Sci. Soc. Am. J.* 63 (1), 55–57.
- Smith, R.E., 2002. Infiltration theory for hydrologic applications. In: Smettem, K.R.J., Broadbridge, P., Woolhiser, D.A., (Eds.), *Water Resources Monograph 15*, American Geophysical Union, Washington, DC, 212 p.
- Trabaud, L., 1994. The effect of fire on nutrient losses and cycling in a *Quercus coccifera* garrigue (southern France). *Oecologia* 99, 379–386.
- Tuller, M., Or, D., 2002. Unsaturated hydraulic conductivity of structured porous media: a review of liquid configuration-based models. *Vadose Zone J.* 1, 14–37.
- Van Genuchten, M.Th., 1980. A closed-form equation for predicting the hydraulic conductivity of unsaturated soils. *Soil Sci. Soc. Am. J.* 44, 892–898.
- Vandervaere, J.-P., Vauclin, M., Elrick, D.A., 2000a. Transient flow from tension infiltrometers: II Four methods to determine sorptivity and conductivity. *Soil Sci. Soc. Am. J.* 64, 1272–1284.
- Vandervaere, J.-P., Vauclin, M., Elrick, D.A., 2000b. Transient flow from tension infiltrometers: I. The two-parameter equation. *Soil Sci. Soc. Am. J.* 64, 1263–1272.
- Wang, Q.-J., Zhang, J.-H., Fan, J., 2006. An analytical method for relationship between hydraulic diffusivity and soil sorptivity. *Pedosphere* 16 (4), 444–450.
- White, I., Sully, M.J., 1987. Macroscopic and microscopic capillary length and time scales from field infiltration. *Water Resour. Res.* 23 (8), 1514–1522.